論文の内容の要旨

論文題目

Carrier Transport in Perovskite-type Oxynitride and
Its Control by Epitaxial Growth Technique

（ペロブスカイト型酸窒化物におけるキャリア輸送と

エピタキシャル成長技術によるその制御）

氏名　佐野　真仁

Introduction

Perovskite-type oxide is one group of metal oxide, and development of new functionality by substitution of their cations has been intensively studied. Recently, substitution of non-metal elements for oxygen attracts attention as a new way to realize novel functionalities. Oxynitride is one group of mixed anion compound, and it has been of interest for its optical properties toward high efficiency photocatalysts and non-toxic pigments with visible light absorption. On the other hand, studies on their intrinsic transport properties have been limited by extrinsic factors originating from the shape of sample, because oxynitride has been conventionally synthesized only in polycrystalline powder form.

To overcome this problem, I fabricated single crystalline oxynitride thin films with d^n ($n \neq 0$) configuration by nitrogen plasma assisted pulsed laser deposition (NPA-PLD) method. The transport properties of the films were analyzed to investigate intrinsic transport properties of perovskite-type oxynitride. Based on the suggested conduction mechanism of perovskite-type oxynitride, next I tried to control its electric transport properties with the following two approaches. First, I fabricated heterostructures composed of oxide and oxynitride layers based on the concept of "remote" doping. Second, I aimed for ordered anion structure to reduce random potential by topotactic nitridation of oxide thin film.

Intrinsic carrier transport properties in perovskite-type oxynitride $LaVO_{3-x}N_x$

For investigation of transport properties of oxynitride, I focused on $LaVO_{3-x}N_x$ (LVON). Its mother material $LaVO_3$ is typical Mott insulator and is known to show insulator-to-metal transition (IMT) by hole-doping through substitution of Ca^{2+} or Sr^{2+} for La^{3+}. In contrast, LVON bulk polycrystal was reported not to show IMT even if a large

number of holes were doped. The mechanism of this carrier localization in LVON was unclear, and influence of extrinsic factors such as grain boundary could not be excluded. To clarify its intrinsic transport properties, LVON epitaxial thin films were fabricated by NPA-PLD method. The deposition was conducted under N_2 gas activated into radicals by a radio frequency plasma source.

Figure 1a compares θ-2θ X-ray diffraction (XRD) patterns of LVON thin films grown at various substrate temperature (T_S). Perovskite-type n00 peaks clearly appeared without any impurity peaks at $T_S \geq 500$ °C while the crystallinity of the thin films were worse at $T_S \leq 450$ °C. The chemical composition of the thin films was evaluated by energy dispersive X-ray (EDX) spectroscopy (Fig. 1b). The monotonic decrease of N peak and increase of O peak against the increase of T_S were apparently observed possibly owing to re-evaporation of N. Therefore, I concluded that T_S = 500 °C was the best for fabrication of single crystalline LVON.

LVON thin films with different nitrogen content were synthesized by varying relative supply rate of nitrogen radical. All films showed only perovskite-type n00 peaks without any impurity peaks, indicating epitaxial growth of LVON within the range of $0 \leq x \leq 0.71$. Their peak position was consistent with the bulk result.

Resistivity (ρ) of the films was evaluated with 4-probe method. A plot of ρ at 300K against nitrogen content (x) is shown in Fig. 2a. ρ of the LVON epitaxial thin films was 2 or 3 orders of magnitude lower than that of bulk polycrystals, indicating suppressed contribution of grain boundaries to ρ. On the other hand, the LVON thin films did not show IMT even for much higher doping level than cation-substituted metallic $LaVO_3$ (Fig. 2b). From the results, I concluded that carrier localization is an intrinsic feature of LVON.

The conduction mechanism of LVON was analyzed from the temperature dependence of ρ by assuming an equation $\rho = \rho_0 \exp(-aT^{\nu})$, where ν is a conduction-model-dependent parameter. Figure 2c shows the $\log[-\partial\ln(\rho)/\partial\ln(T)]$ vs $\log(T)$ plot for the LVON thin film with the highest nitrogen content (x = 0.71), the slope of which gives ν. The plot indicates $\nu = -1$ and $\nu = -1/2$ in a range of $T > 170$ K and $T < 170$ K, respectively. $\nu = -1$ at high temperature suggests the dominance of thermally activated band conduction or nearest neighbor hopping conduction, although it is difficult to distinguish them. On the other hand, $\nu = -1/2$ at low temperature has not been completely explained theoretically, while the same behavior has been observed experimentally for the materials in which strong electron correlation and large disorder coexist [4]. Therefore, I concuded that strongly disordered potential induced by random substitution of N for O contributes to the carrier localization in LVON. Because N in perovskite-type oxynitride tends to occupy the

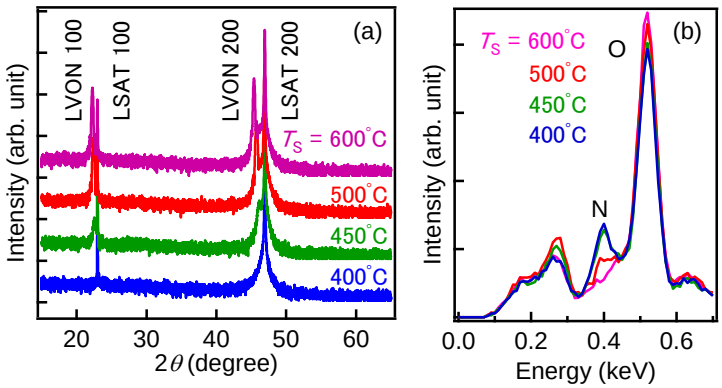

Figure 1. (a) θ-2θ XRD patterns and (b) EDX spectra of the LVON films grown on LSAT (100) substrates at various T_S.

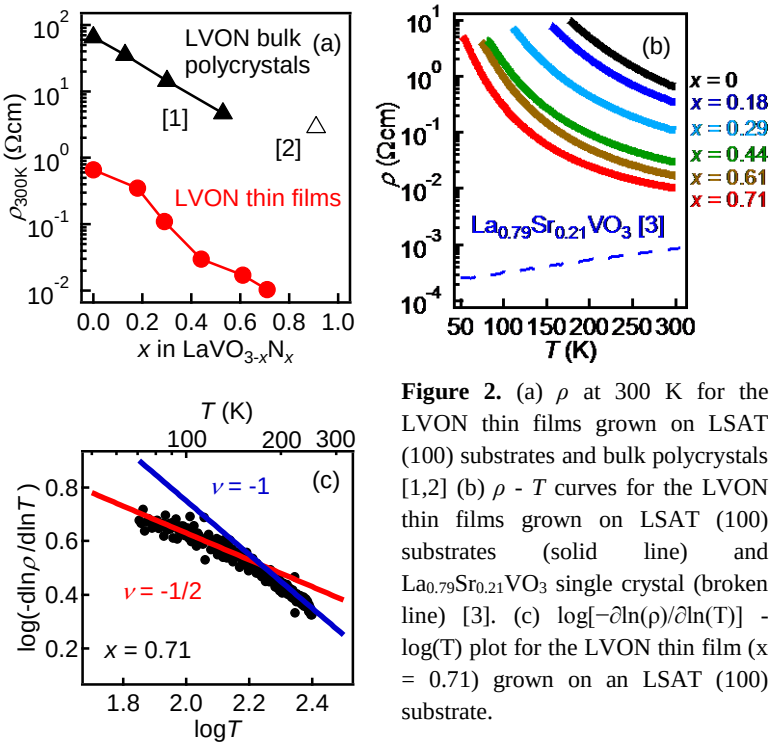

Figure 2. (a) ρ at 300 K for the LVON thin films grown on LSAT (100) substrates and bulk polycrystals [1,2] (b) ρ - T curves for the LVON thin films grown on LSAT (100) substrates (solid line) and $La_{0.79}Sr_{0.21}VO_3$ single crystal (broken line) [3]. (c) $\log[-\partial\ln(\rho)/\partial\ln(T)]$ - log(T) plot for the LVON thin film (x = 0.71) grown on an LSAT (100) substrate.

anion site randomly, large contribution of anion disorder to carrier localization would be a general feature of perovskite-type oxynitrides.

Formation of oxide/oxynitride superlattice for remote doping

As discussed above, the transport properties of oxynitride might be largely influenced by disordered potential. Thus, if the holes doped into oxynitride can penetrate into adjacent undoped layer, it is possible to reduce the influence of the disordered potential and to enhance the conductivity at oxide/oxynitride interface. This concept of "remote" doping has been realized in oxide superlattice structures [5]. Based on this idea, I tried remote hole doping from $LaVO_{3-x}N_x$ layer into $LaVO_3$ layer by forming superlattice structure of them.

$[(LaVO_3)_m/(LaVO_{2.5}N_{0.5})_m]_n$ (m = 10, n = 4 and m = 5, n = 8) single crystalline superlattices were epitaxially fabricated on (100) plane of $SrTiO_3$ (STO) and (001) plane of $NdGaO_3$ (NGO) substrates. The oxide and oxynitride layers were alternately deposited with closing and opening the shutter attached in front of the radical source. Their XRD patterns showed clear satellite peaks consistent with the periodicity of designed superlattice structures. Secondary ion mass spectroscopy (SIMS) confirmed periodic anion distribution (Fig. 3), although a finite amount of nitrogen was detected in the oxide layer possibly owing to nitrogen leakage through the closed shutter. The superlattice showed the conductance higher than that estimated only from the bulk conductions (Fig. 4), suggesting the contribution of remote doping to the conduction of superlattice structure. I also fabricated $(LaVO_3)_{10}/(LaVO_{2.6}N_{0.4})_{10}$ single-heterostructure, for which composition with higher precision was expected. The conductance measurement of the single-heterostructure supported the contribution of remote doping. This study suggests that the conductivity of perovskite-type oxynitride may be enhanced by forming gradation in N distribution.

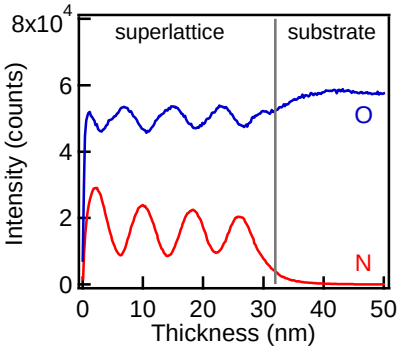

Figure 3. Depth profile of the $[(LaVO_3)_{10}/(LaVO_{2.5}N_{0.5})_{10}]_4$ superlattice grown on an STO (100) substrate, measured by SIMS.

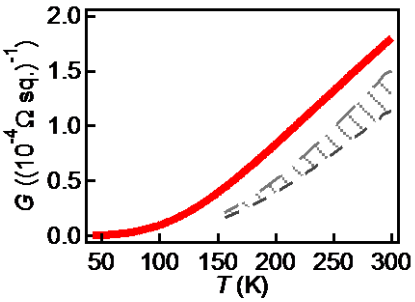

Figure 4. The sheet conductance (G) of the superlattice grown on an NGO (001) substrate (red) plotted as functions of temperature. The area shown by oblique lines indicates possible region of G for the superlattice assuming only bulk conductions.

Topotactic nitridation of layered perovskite oxide for anion-ordered structure

As discussed above, disordered potential introduced by random substitution of N localizes the carriers in oxynitrides. In other words, ordered anion configuration could enhance carrier conduction without formation of stacked structure. In the case of ABO_2N-type perovskite oxynitrides, *cis*- and *trans*-type local configurations are possible. In bulk ones, generally, the *cis*-type local configuration is more stable, and complicated *cis*-network without long-range ordering is formed.

To achieve long-range anion ordering, I focused on topotactic nitridation of layered perovskite (LP) oxide. Some LP oxide can be nitrided to perovskite-type oxynitride with ammonolysis method. In the reaction, nitrogen substitution predominantly proceeds along the excess oxygen layers [6], which is linear to <110> direction for perovskite-type structure. It suggests that long-range *cis*-ordering might be obtained by nitridation of epitaxial LP oxide thin films with single crystallographic orientation. LP-$La_2Ti_2O_7$ and $Sm_2Ti_2O_7$ thin films were epitaxially grown on (110) planes of STO and LSAT substrates. Among them, $La_2Ti_2O_7$ was grown with (100)- and (010)-orientation, of which excess oxygen layers are parallel and perpendicular to the film surface, respectively, owing to the lattice mismatch on each

substrate. After the ammonolysis process (1000 °C, 1 hour), the LP-$La_2Ti_2O_7$ thin films were converted to perovskite-type $LaTiO_2N$, while the substrates were not nitrided (Figs. 5b and 5c). Only 110 peaks of $LaTiO_2N$ appeared in the XRD patterns, suggesting that the reaction was topotactic one. Therefore, this synthesis route is confirmed as one effective method to obtain single crystalline perovskite-type oxynitride thin film. The XRD patterns, however, did not show any peaks corresponding to anion-ordered structure. Furthermore, the peak positions were totally coincide between the films synthesized from (100)- and (010)-oriented precursors. These results indicate random substitution of nitrogen for oxygen, probably because high reaction temperature required for ammonolysis caused random nitrogen diffusion together with along the excess oxygen layers.

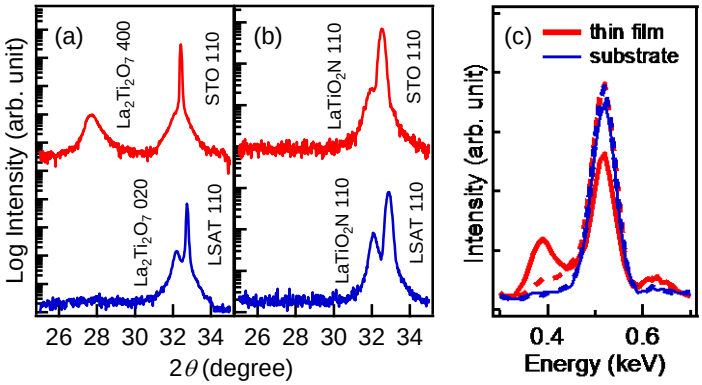

Figure 5. XRD patterns of (a) the precursors and (b) the reacted samples grown on STO (110) (red) and LSAT (110) (blue) substrates. (c) EDX spectra of the thin film and LSAT substrate before (dashed) and after (solid) ammonolysis.

Summary

I investigated intrinsic transport properties of perovskite-type oxynitride by using NPA-PLD method and developed multiple applications of epitaxial growth techniques toward control of its transport properties. Perovskite-type $LaVO_{3-x}N_x$ single crystalline thin films were grown, and resistivity measurements of the films revealed strong carrier localization due to random substitution of nitrogen for oxygen. This result indicates that reduction of disordered potential would drastically change the transport properties of oxynitride. As one approach for control of the transport properties, remote hole doping from oxynitride to adjacent oxide layer was performed with oxide/oxynitride superlattice and single-heterostructure. From their conductance measurements, enhancement of the conductivity owing to remote doping was suggested. As another approach, I tried to synthesize anion-ordered oxynitrides by using topotactic nitridation of single-oriented LP precursor. This process was established as one route to fabricate single crystalline perovskite-type oxynitride thin film, although there remains some room for optimization to suppress thermal diffusion of N.

I also tried to achieve ordered anion arrangement by applying epitaxial strain on the crystal lattice. Large tetragonal strain was introduced in $LaTiO_2N$ thin film, for which partial trans-type long-range anion ordering is expected.

References

[1] P. Antoine *et al.*, *Mater. Sci. Eng.* B **5**, 43 (1989). [2] J. Oro-Sole *et al.*, *J. Mater. Chem.* C **2**, 2212 (2014). [3] S. Miyasaka *et al.*, *Phys. Rev. Lett.* **85**, 5388 (2000). [4] S. Nakatsuji *et al.*, *Phys. Rev. Lett.* **93**, 146401 (2004). [5] A. Ohtomo *et al.*, *Nature* **419**, 378 (2002). [6] M. Yang *et al.*, *Nat. Chem.* **3**, 47 (2011). [7] S. G. Ebbinghaus *et al.*, *Solid State Sciences* **10**, 709 (2008).